Chemosphere 250 (2020) 126305

Contents lists available at ScienceDirect

Chemosphere

journal homepage: www.elsevier.com/locate/chemosphere

Low-concentration tracer tests to measure air-water interfacial area in porous media

Mark L. Brusseau [a, b, *], Ying Lyu [c], Ni Yan [d], Bo Guo [b]

[a] Environmental Science Department, University of Arizona, Tucson, AZ, 85721, USA
[b] Hydrology and Atmospheric Science Department, University of Arizona, Tucson, AZ, 85721, USA
[c] Institute of Water Resources and Environment, College of Construction Engineering, Jilin University, Changchun, 130026, PR China
[d] Key Lab of Marine Environmental Science and Ecology, Ministry of Education, College of Environmental Science and Engineering, Ocean University of China, Qingdao, 266100, PR China

HIGHLIGHTS

- A modified tracer test method is presented to measure air-water interfacial areas.
- The method is not affected by tracer-induced drainage.
- Robust air-water interfacial areas were measured that increased with decreasing water saturation.

ARTICLE INFO

Article history:
Received 10 January 2020
Received in revised form
13 February 2020
Accepted 20 February 2020
Available online 22 February 2020

Handling Editor: Keith Maruya

Keywords:
Interfacial partitioning
Interfacial adsorption
Fluid-fluid interfaces

ABSTRACT

The aqueous-based interfacial tracer method employing miscible-displacement tests is one method available for measuring air-water interfacial areas. One potential limitation to the method is the impact of tracer-induced drainage on the system. The objective of this study was to investigate the efficacy of a low-concentration tracer test method for measuring air-water interfacial area. Tracer concentrations and analytical methods were selected that allowed the use of tracer input concentrations that were below the threshold of tracer-induced drainage. Multiple tracer tests were conducted at different water saturations. Interfacial areas increased from 34.8 to 101 cm^{-1} with the decrease in saturation from 0.86 to 0.62. The method produced relatively robust measurements of air-water interfacial area, with coefficients of variation ranging from 6 to 26%. A variably saturated flow and transport model that accounts for the effects of tracer on interfacial tension, and the retention of tracer at the air-water and solid-water interfaces, was used to test for potential tracer-induced drainage. The simulations showed that the use of low tracer-input concentrations eliminated this phenomenon. This is consistent with the measured data for effluent-sample masses, which exhibited minimal change during the tests, and with the observation that the interfacial areas obtained with the low-concentration-tracer method were consistent with values measured with two methods that are not influenced by tracer-induced drainage. These results demonstrate that the low-concentration miscible-displacement tracer test method is an effective approach for measuring air-water interfacial areas in porous media.

1. Introduction

The significance of the interfaces between immiscible fluids has long been recognized in several fields of study. For example, the air-water interface in unsaturated porous media plays a role in two-phase flow, soil shear strength and compressibility, mass-transfer processes, and the retention of colloidal and dissolved contaminants. Full examination and characterization of air-water interfacial phenomena requires methods of measurement. Two primary approaches have been developed to measure air-water interfacial area in porous media, imaging-based methods and tracer-test methods.

High-resolution 3-D imaging methods based on x-ray absorption microtomography (XMT) have been developed over the past 15 years. XMT has been used to measure air-water interfacial areas for

* Corresponding author. Environmental Science Department, University of Arizona, Tucson, AZ, 85721 USA.
E-mail address: brusseau@email.arizona.edu (M.L. Brusseau).

https://doi.org/10.1016/j.chemosphere.2020.126305
0045-6535/

Table 1
Properties of interfacial tracers.

Tracer	**MW** (g/mol)	**Aqueous Solubility** (g/L; 25 °C)	**Critical Micelle Concentration**[b] (g/L)
PFDA	414	9.5[a]	4
APMO	347	>10	>10

[a] From Kauck and Diesslin (1951)..
[b] In 0.01 M NaCl solution.

Table 2
Tracer test conditions.

Water Saturation	Input Concentration (mg/L)	Tracer	Number of Tests
0.62	1 and 0.01	APMO	3
0.68	1, 0.1, and 0.01	PFDA and APMO	7
0.74	1	PFDA	1
0.77	1	PFDA	3
0.86	1	PFDA	1

synthetic and natural porous media (Culligan et al., 2004; Brusseau et al., 2006, 2007; Costanza-Robinson et al., 2008; Araujo and Brusseau, 2019; Lyu et al., 2017; Willson et al., 2012). An advantage of this method is the ability to differentiate between capillary and film-associated interfaces. One disadvantage of this method is that the contribution of surface roughness to film interfacial area is not fully captured due to resolution constraints (Brusseau et al., 2006, 2007). Hence, total air-water interfacial areas measured with XMT are typically lower than true values.

Several methods have been developed that employ a surface-active (i.e., interfacial) tracer to measure air-water interfacial area based on observed retention of the tracer. These methods determine effective interfacial areas that are a function of the specific method. They provide measures of total interfacial area, incorporating contributions from capillary and film-associated interfaces. They typically provide some measure of roughness-associated film interfacial area.

Rao and colleagues (Saripalli et al., 1997; Kim et al., 1997) introduced an aqueous-based interfacial tracer method employing miscible-displacement tests. One potential limitation to the method is the impact of the interfacial tracer on surface tension of solutions within the packed column. The reduction in surface tension upon introduction of the tracer solution can cause water flow and drainage, as discussed by Kim et al. (1997). This phenomenon can under certain conditions create uncertainty in the measured water saturations and interfacial areas (Costanza-Robinson et al., 2012).

Alternative tracer methods have been developed and used to measure air-water interfacial area, including mass-balance methods (Anwar et al., 2000; Schaefer et al., 2000; Anwar, 2001; Araujo et al., 2015) and gas-phase tracer-test methods (Brusseau et al., 1997; Kim et al., 1999, 2001; Costanza-Robinson and Brusseau, 2002; Peng and Brusseau, 2005). However, the standard miscible-displacement method remains a useful approach as it produces measurements under conditions most representative of water flow and solute transport in porous media. Thus, the interfacial areas determined with this method may be most representative for characterizing mass-transfer and contaminant-retention processes for aqueous-based transport. It is of interest then to develop modified approaches for this method that eliminate the issue of tracer-induced drainage and its attendant potential impacts on measured interfacial areas.

The objective of this study is to investigate the efficacy of a low-concentration tracer test method for measuring air-water interfacial area in porous media. Tracer concentrations and analytical methods are selected that allow the use of tracer input concentrations that are below the threshold of tracer-induced drainage. Multiple tracer tests are conducted at different water saturations. The measured interfacial areas are compared to values obtained with XMT and alternative tracer-based methods. A variably saturated flow and transport model that accounts for the effects of tracer on interfacial tension, and the retention of tracer at the air-water and solid-water interfaces, is used to test for potential tracer-induced drainage.

2. Materials and methods

2.1. Materials

Pentafluorobenzoic acid was used as the nonreactive tracer (NRT). Pentadecafluorooctanoic acid (PDFA; 98% purity purchased from AIKE Reagent) and ammonium perfluoro(2-methyl-3-oxahexanoate) (APMO; 95% purity purchased from Manchester Organics), both surfactants, were used as the interfacial tracers. Select properties of these two compounds are reported in Table 1. Sodium chloride (0.01 M) was used as the background electrolyte solution for all experiments. Solutions were prepared using distilled, deionized water. Natural quartz sand with a mean diameter of 0.35 mm was used for the tracer tests. It has an air-entry matric potential of 14.6 cm. It has no measurable clay mineral content and very low organic-carbon and metal-oxide contents. The medium exhibits no adsorption of the NRT and a very low magnitude of adsorption for the interfacial tracers.

The columns were constructed of acrylic and were 15 cm long with an inner diameter of 2 cm. Flow distributors were placed in contact with the porous media on the top and bottom of the column to help promote uniform fluid distribution and to support the media. Peristaltic pumps were used to provide fluid flow.

2.2. Methods

The surface tensions of aqueous PFDA and APMO solutions (with 0.01 M NaCl) were measured using a De Nouy ring tensionmeter (Fisherscientific, Surface Tensiomat 21) following standard methods (ASTM D1331- 89). The tensiometer was calibrated with a weight of known mass. Each sample was measured three times with the deviation between measurements less than ~1%.

The miscible-displacement tracer tests were conducted using methods we have used in previous studies (cf., Brusseau et al., 2007, 2015; Lyu et al., 2018). These methods have been demonstrated to

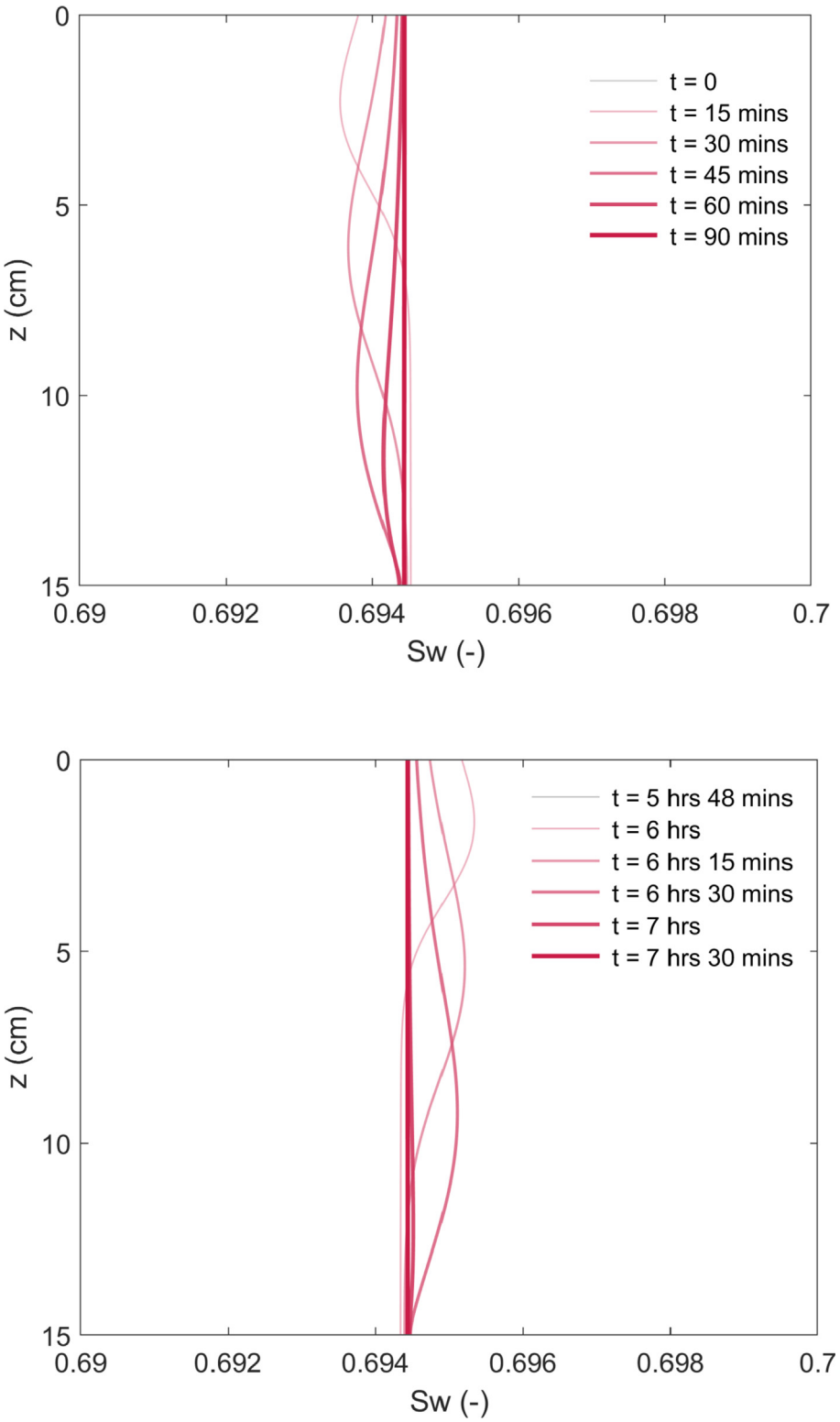

Fig. 1. Simulated water saturation distribution along the column profile for different times after tracer-solution injection (top) or displacement (bottom). Elution starts at 5 h 48 min.

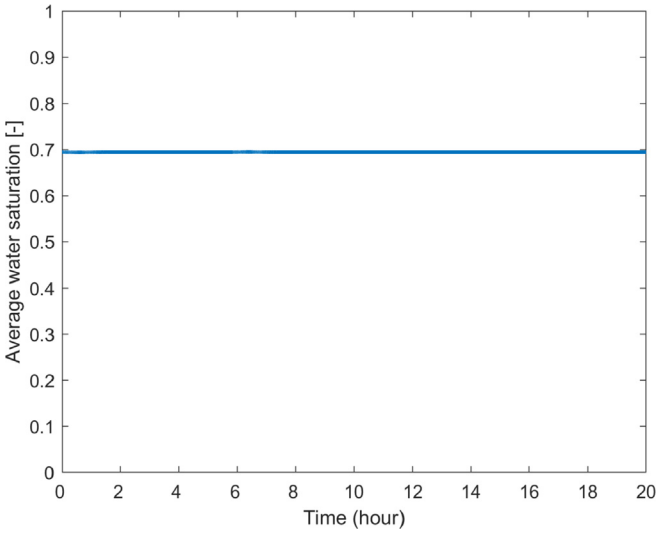

Fig. 2. Simulated mean water saturation within the column.

produce steady-state water flow and uniform distributions of water for unsaturated conditions. The columns were oriented vertically for all experiments. The experiments were conducted at room temperature (25±1 °C).

Each column was packed with air-dried sand to a uniform bulk density (~1.5 g/cm^3). Electrolyte solution was then pumped into the bottom of the column at a low flow rate until the column was saturated. Tracer tests with the NRT and the interfacial tracers were then conducted. The latter tests provide determination of adsorption of the tracers by the sand. The columns were then drained to a target water saturation, and tracer tests were conducted to measure air-water interfacial area. The column was weighed before saturation, after saturation, and after drainage to determine bulk density, porosity, and water content. Different water saturations and tracer-input concentrations were used for the tests (see Table 2). Some of the raw breakthrough-curve data analyzed herein were reported previously (Lyu et al., 2018); however, these data were not processed in that work to determine air-water interfacial areas.

Samples of column effluent were collected in polypropylene tubes and analyzed immediately after collection. The NRT was analyzed by ultraviolet−visible (UV−Vis) spectrophotometry. PDFA and APMO were analyzed by high-performance liquid chromatography and mass spectrometry, i.e., LC-MS. The column was a C18 maintained at 40 °C. The dual mobile phase comprised ammonium acetate and either acetonitrile (PDFA) or methanol (APMO) applied in a gradient at a flow rate of 0.2 mL/min. The aqueous samples were injected directly, with injection volumes of ~2 μL. Retention times were consistent at ~4.3 and 1 min for PDFA and APMO, respectively. Standard QA/QC protocols were employed. Blanks, background samples, and check standards were analyzed periodically for each sample set. The results for the first two were lower than the quantifiable detection limit. The calibration curve attained a coefficient of determination (r^2) larger than 0.999. The quantifiable detection limits were ~0.2 μg/L.

2.3. Data analysis

The retardation factor for aqueous-phase transport of an interfacial tracer under water-unsaturated conditions is defined as (e.g., Kim et al., 1997; Brusseau et al., 2007):

$$R = 1 + K_d\rho_b/\theta_w + K_iA_i/\theta_w \quad (1)$$

Where K_d is the solid-phase adsorption coefficient (cm^3/g), K_i is the air-water interfacial adsorption coefficient (cm^3/cm^2), A_i is the specific air-water interfacial area (cm^2/cm^3), ρ_b is porous-medium bulk density (g/cm^3), and θ_w is volumetric water content (−). Values for A_i are determined from the measured breakthrough curves for the interfacial tracer by solving equation (1), with all other variables known. Measured retardation factors are determined from the breakthrough curves by the standard method of moments. The value for K_d is obtained from the saturated-flow tracer test. The value for K_i is obtained from measured surface tension data. The values for ρ_b and θ_w are measured for each test.

The K_i can be determined from measured surface tension data by (e.g., Kim et al., 1997; Brusseau et al., 2007):

$$K_i = \frac{\Gamma}{C} = \frac{-1}{RTC}\frac{\partial\gamma}{\partial \ln C} \quad (2)$$

where γ is the surface tension (mN/m), C is the aqueous phase concentration (mol/cm^3), Γ (mol/cm^2) is the surface excess, is temperature (°K), and R is the gas constant (erg/mol °K). The Szyszkowski equation was applied to the surface tension data to provide a uniform means of calculating K_i values. It has been widely demonstrated that this equation provides accurate representation of surface tension data for all types of surface-active constituents (e.g., Adamson, 1982; Barnes and Gentle, 2005). One form of the equation is given as (e.g., Adamson, 1982; Barnes and Gentle, 2005):

$$\gamma = \gamma_0\left[1 - B\,ln\left(1 + \frac{C}{A}\right)\right] \quad (3)$$

where γ_0 is the interfacial tension at C = 0 (e.g., the surface tension of pure water), and *A* and *B* are variables related to properties of the specific compound and of the homologous series, respectively. The best-fit functions were used to obtain the local-slope factors required for equation (2).

2.4. Mathematical modeling

A numerical model that couples transient variably saturated flow and tracer transport (Guo et al., 2020) was used in preliminary simulations to investigate the potential for tracer-induced drainage for the conditions of the experiments. The model simulates the impact of an interfacial tracer on surface tension, and the subsequent influence on displacement of the solution. The model also simulates transport of the interfacial tracer, and explicitly accounts for nonlinear adsorption at the solid-water and air-water interfaces. The coupled equations of flow and transport are solved by a fully implicit numerical framework using Newton-Raphson iterations. Details of the equations and numerical methods are provided in Guo et al. (2020).

3. Results and discussion

3.1. Numerical simulation

A one-dimensional simulation is performed in the present study to examine whether tracer-induced drainage and flow is relevant for the tracer tests. The domain is vertical with a length of 15 cm and is discretized into 300 numerical cells with a uniform size. The top boundary is set as constant flux with an infiltration rate of 0.16 cm/min. The bottom boundary is set as free drainage. Initially, the domain is under steady-state flow with a flow rate of 0.16 cm/min. The interfacial tracer solution with a concentration of 1 mg/L is

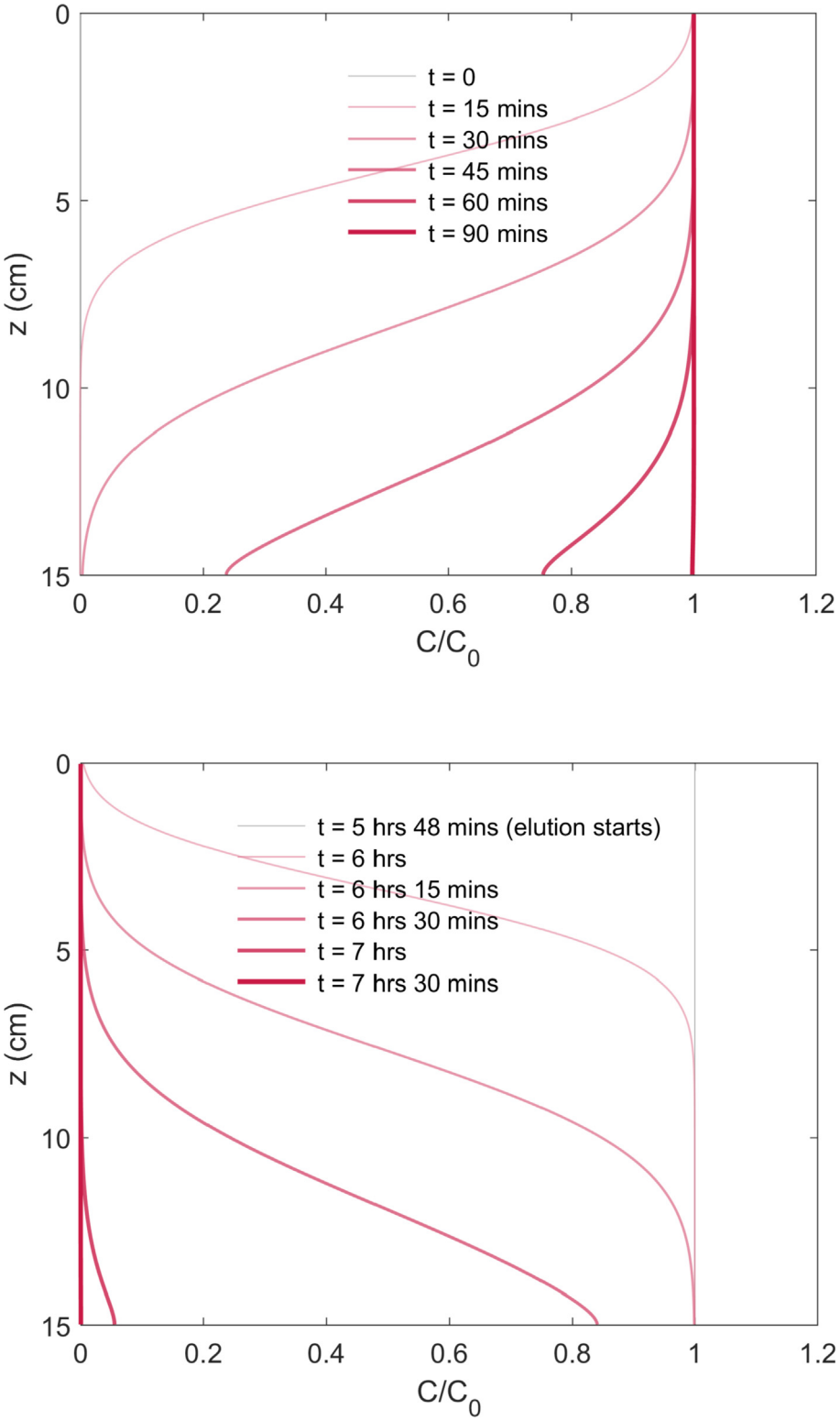

Fig. 3. Simulated tracer concentration profiles for different times after tracer-solution injection (top) or displacement (bottom).

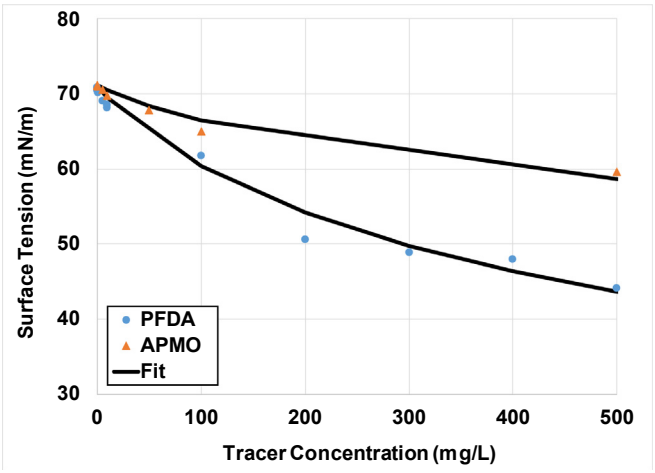

Fig. 4. Measured and fitted (Szyszkowski equation) surface tensions for the two interfacial tracers.

applied at time zero and stopped at t = 5 h 48 min. The simulation lasts for 20 h. Other parameters used for the simulation include saturated hydraulic conductivity $K_{sat} = 1.26$ cm/min, porosity $n = 0.36$, residual water content $\theta_r = 0.015$, diffusion coefficient $D_m = 4.9 \times 10^{-6}$ cm^2/s, longitudinal dispersivity $\alpha_L = 0.29$ cm, solid-phase adsorption coefficient $K_d = 0.08$ cm^3/g, bulk density $\rho_b = 1.5$ g/cm^3. The soil water characteristic curve and relative permeability is modeled by the van Genuchten model with the parameters $\alpha = 0.0448$ cm^{-1}, $n = 4$, and $m = 0.75$. The air-water interfacial area is represented as a function of water saturation based on aggregated measurements reported in Jiang et al. (2020). The surface tension γ and K_i are determined using measured surface tension data for PDFA, the tracer with greater surface activity.

The results of the mathematical modeling show that the water saturation within the column changes by less than 0.001, equivalent to ~0.1%, upon introduction or displacement of the tracer solution (Fig. 1). As a result, the mean water saturation within the entire column did not change during the course of the tracer tests (Fig. 2). In addition, solution-concentration profiles of the tracer within the column are ideal (Fig. 3). These results demonstrate the absence of tracer-induced drainage effects. The simulation was conducted with an input concentration of 1 mg/L, the largest value used for the tracer tests. Thus, the interfacial areas measured with this method are free from tracer-induced drainage effects at all input concentrations employed.

3.2. Surface tension data

The surface tensions of the two tracers in electrolyte solution are presented in Fig. 4. The surface activity of PDFA is greater than that of APMO, consistent with its longer carbon chain (e.g., Traube's Rule). These data were used to determine K_i values for the relevant concentrations, which are reported in Table 3.

The K_i values for the two tracers determined from the surface-tension data as a function of concentration are presented in Fig. 5. The data show that the values are essentially constant at

Table 3
Adsorption coefficients.

Input Concentration (mg/L)	K_i – PDFA (cm)	K_i – APMO (cm)	K_d – PDFA (cm^3/g)	K_d – APMO (cm^3/g)
1	0.00261	0.00095	0.075	0.016
0.1	0.00263	–	0.094	–
0.01	0.00268	0.00096	0.12	0.029

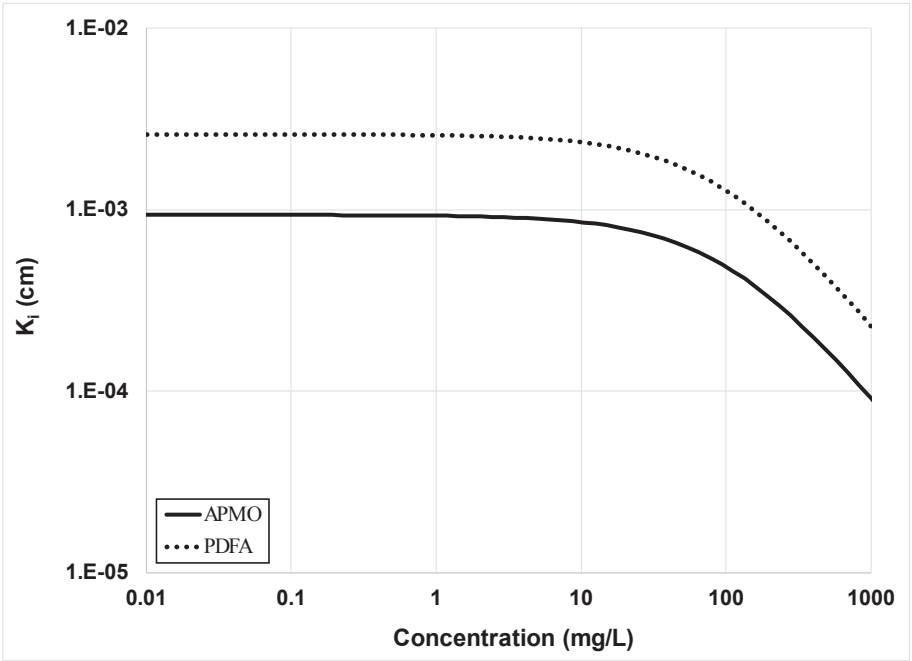

Fig. 5. Air-water interfacial adsorption coefficient (K_i) as a function of tracer concentration.

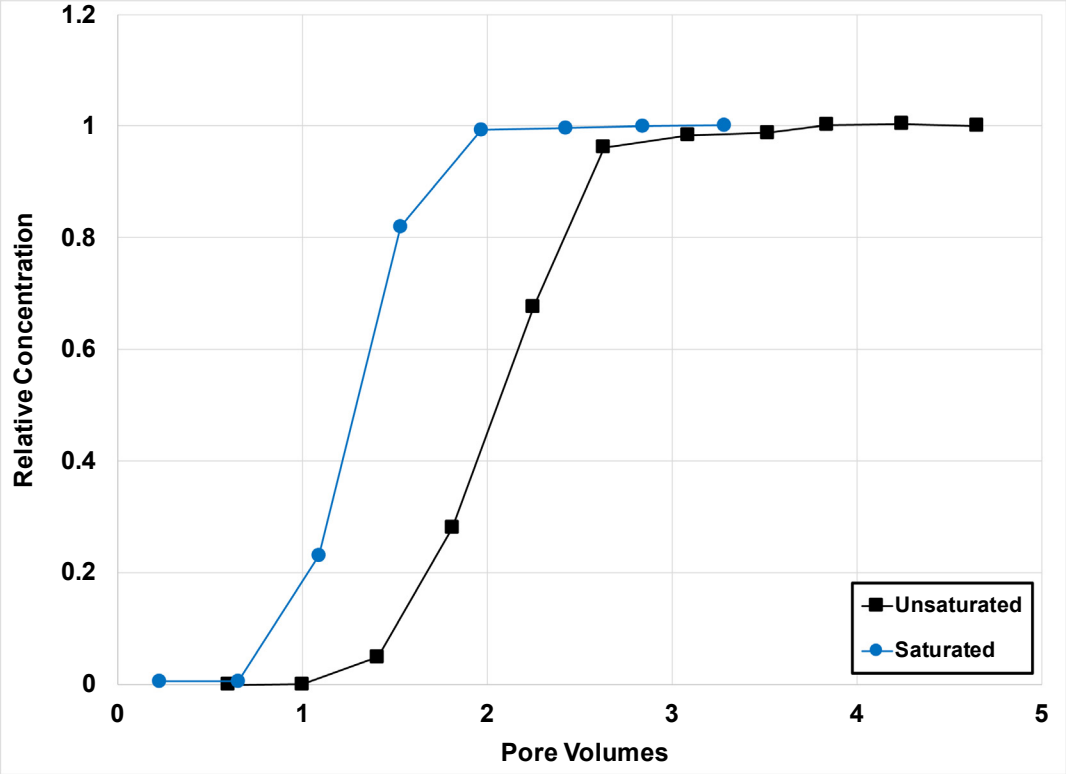

Fig. 6. Breakthrough curves for PFDA transport in sand under saturated and unsaturated (S_w = 0.68) conditions. Relative concentration represents the effluent concentration divided by the input concentration; pore volume represents the effluent discharge divided by the water volume retained by the packed column.

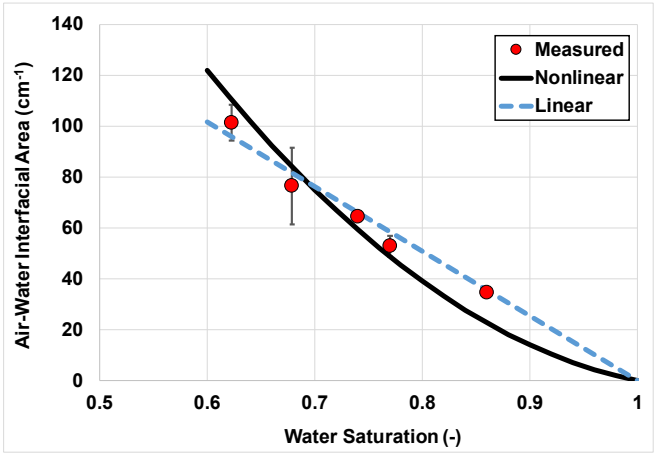

Fig. 7. Air-water interfacial areas measured with the low-concentration tracer-test method.

concentrations below 1 mg/L. The K_i for PDFA is approximately 2.5 times larger than that for APMO. This again is consistent with the longer carbon chain of PDFA.

3.3. Tracer tests

The breakthrough curves for the nonreactive tracer exhibited ideal transport behavior for both saturated and unsaturated conditions (data not shown), indicating uniform packing and flow conditions. The retardation factors for PDFA and APMO under saturated flow ranged from 1.1 to 1.2. These low values are consistent with a small degree of adsorption by the sand. The K_d values determined for PDFA and APMO are reported in Table 3. The values for both tracers are larger for lower concentrations, indicating the influence of nonlinear adsorption. The K_ds are larger for PDFA compared to APMO, consistent with their molecular structure.

The breakthrough curves for PDFA and APMO under unsaturated flow exhibit greater retardation compared to saturated flow, due to the additional retention at the air-water interface. An illustrative example is provided in Fig. 6. Retardation factors range from 1.8 to 2.8 for PDFA and 1.3 to 1.5 for APMO, depending upon the water saturation. The contribution of air-water interfacial adsorption to total retention ranges from 50 to 80% for both tracers. Higher contributions are associated with lower water saturations due to the larger air-water interfacial areas present.

The high relative contributions of air-water interfacial adsorption to retardation allow PDFA and APMO to serve as effective tracers for characterizing air-water interfacial area in this medium. As noted above, the K_d values for both tracers for the sand are relatively low. This is a result of the minimal quantities of organic carbon, metal oxides, and clay minerals present in the sand. Application of the tracers for porous media with significantly larger quantities of these constituents would likely result in larger magnitudes of solid-phase adsorption, and a reduction in the relative contribution of air-water interfacial adsorption to total retardation. If the relative contribution becomes sufficiently small to reside within the experimental uncertainty, the tracers would no longer be effective for measuring air-water interfacial area.

3.4. Air-water interfacial areas

The measured air-water interfacial areas are reported in Fig. 7. Their magnitude is observed to increase for smaller water saturations, consistent with prior measurements of total air-water interfacial area (e.g., Kim et al., 1997; Anwar et al., 2000; Schaefer

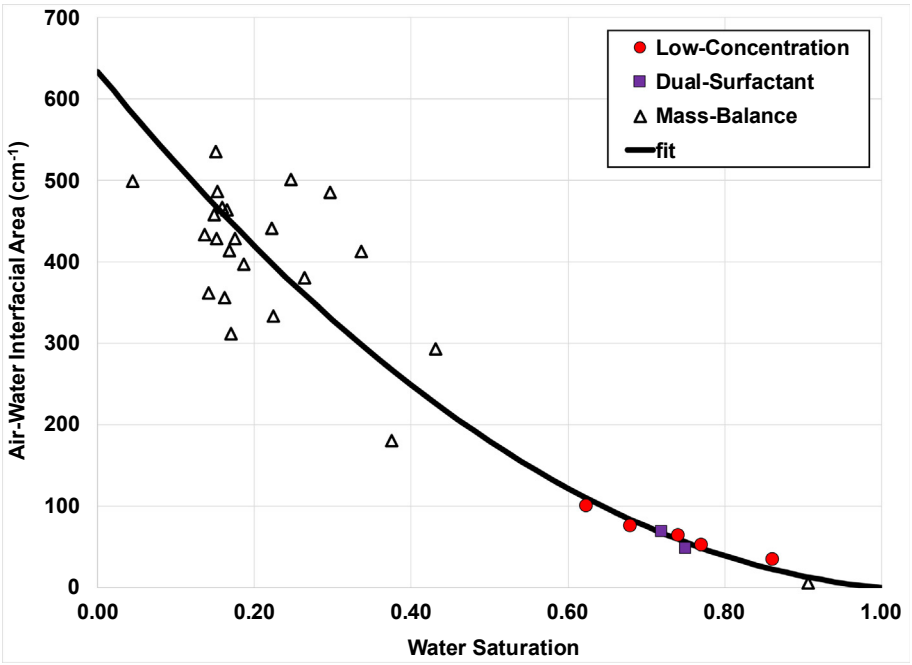

Fig. 8. Air-water interfacial areas measured with the low-concentration tracer-test method compared to values measured with the dual-surfactant method (data from Brusseau et al., 2015) and the mass-balance method (data from Araujo et al., 2015).

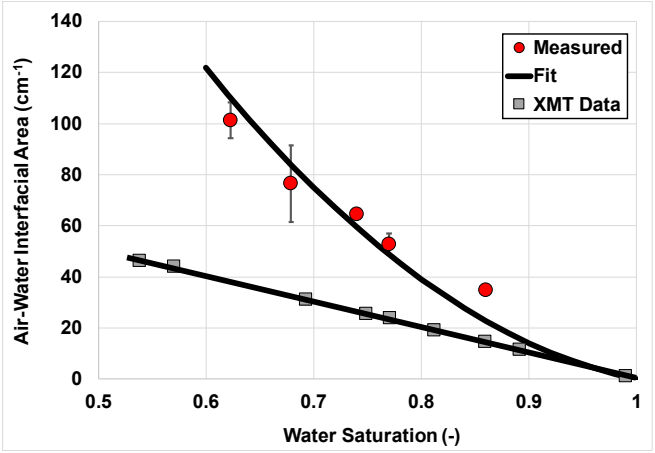

Fig. 9. Air-water interfacial areas measured with the low-concentration tracer-test method compared to the x-ray microtomography (XMT) method. The XMT data were reported in Lyu et al. (2017).

et al., 2000; Anwar, 2001; Brusseau et al., 2007; Araujo et al., 2015). The degrees of uncertainty for the points with multiple measurements are relatively small, with coefficients of variation of 6, 7, and 26%. These are within the ranges reported for prior interfacial tracer-test studies (Dobson et al., 2006; Brusseau et al., 2008).

Inspection of Fig. 7 shows that nonlinear and linear functions both produce reasonable fits to the measured data. Total air-water interfacial areas measured with XMT exhibit linear increases with decreasing water saturation (Brusseau et al., 2006, 2007; Costanza-Robinson et al., 2008; Lyu et al., 2017; Araujo and Brusseau, 2019). Conversely, air-water interfacial areas measured with gas-phase interfacial tracer tests exhibit nonlinear, exponential increases with decreasing water saturation (Kim et al., 1999, 2001; Costanza-Robinson and Brusseau, 2002; Peng and Brusseau, 2005). This behavior is also demonstrated in simulations produced with pore-scale models that account for film-associated interfacial area (Or and Tuller, 1999; Jiang et al., 2020). Such behavior is in part a result of surface roughness impacts on film-associated interfacial area, as discussed in the cited papers.

The air-water interfacial areas measured with the low-concentration tracer-test method are compared to data obtained with two other tracer-based methods in Fig. 8. Araujo et al. (2015) used the mass-balance tracer method to measure air-water interfacial areas for a 0.35-mm quartz sand. Brusseau et al. (2015) used a miscible-displacement dual-surfactant tracer-test method to measure air-water interfacial areas for a 0.35-mm quartz sand. As discussed by the authors, the design of these two methods eliminates tracer-induced drainage.

Inspection of Fig. 8 shows that the interfacial areas measured with the low-concentration tracer-tests are quite consistent with those obtained with the other two methods. This consistency is further evidence that tracer-induced drainage effects did not influence the low-concentration tracer-test method. This is supported further by the minimal changes (average ~4%) observed for effluent sample masses for the experiments, which is within the flow-rate variability of the pumps. The consistency between the low-concentration-tracer values and the mass-balance values also indicates that any impact of potential interfacial mobility on the measured interfacial areas obtained with the former method is negligible, given that such effects do not influence the mass-balance method. Combining the three sets of data shows that a nonlinear function provides a better match to the measured data over the entire range of water saturation.

It is noted that the mass-balance method produces somewhat noisy data for natural media (Araujo et al., 2015), as also observed in the data reported by Schaefer et al. (2000). This is a potential limitation of the method. A limitation of the dual-surfactant method is the need to match the surface activities and solid-phase adsorption of the two interfacial tracers, which may become difficult for very geochemically heterogeneous media. The low-concentration tracer-test method is not constrained by these limitations. However, the method remains labor-intensive, as are all

miscible-displacement methods.

Air-water interfacial areas measured with the low-concentration tracer-test method are compared in Fig. 9 to total air-water interfacial areas measured with XMT. The values measured with XMT are clearly significantly smaller than those measured with the interfacial tracer test. This is consistent with the results of prior comparisons (Brusseau et al., 2007, 2008; McDonald et al., 2016). This disparity is related to the resolution constraints of the XMT method and its inability to characterize the contribution of roughness-associated film interfacial area.

4. Conclusion

The low-concentration tracer-test method produced robust measurements of air-water interfacial area. The tracer tests were conducted with input concentrations of 1, 0.1, and 0.01 mg/L. Tracer-input concentrations are typically 30–400 mg/L for the standard miscible-displacement tracer-test method. Mathematical modeling conducted with a variably saturated flow and transport model that accounts for tracer-induced drainage showed that the use of low tracer-input concentrations eliminated this phenomenon. Interfacial areas measured with the low-concentration tracer-test method were very consistent with interfacial areas obtained with two other tracer-based methods that by design are not influenced by tracer-induced drainage. These results demonstrate that the low-concentration tracer-test method is an effective approach for measuring air-water interfacial areas in porous media.

Declaration of competing interests

The authors declare that they have no known competing financial interests or personal relationships that could have appeared to influence the work reported in this paper.

CRediT authorship contribution statement

Mark L. Brusseau: Conceptualization, Methodology, Writing - original draft. **Ying Lyu:** Data curation, Writing - review & editing. **Ni Yan:** Data curation, Writing - review & editing. **Bo Guo:** Writing - review & editing.

Acknowledgements

This work was supported by the NIEHS Superfund Research Program (grant no. P42 ES04940). Additional funding for Dr. Ying Lyu was provided by the National Natural Science Foundation of China (NO. 41902247) and China Postdoctoral Science Foundation (NO. 2018M640284). We thank the reviewers for their constructive comments.

References

Adamson, A.W., 1982. Physical Chemistry of Surfaces, fourth ed. J. Wiley, New York.
Anwar, A.H.M.F., 2001. Experimental determination of air-water interfacial area in unsaturated sand medium. In: Seiler, K.-P., Wohnlich, S. (Eds.), New Approaches Characterizing Groundwater Flow: Proceedings of XXXI IAH Congress, Munich, Germany, vol. 2. Taylor & Francis, Abingdon, UK, pp. 821–825.
Anwar, A.H.M.F., Bettahar, M., Matsubayashi, U., 2000. A method for determining air-water interfacial area in variably saturated porous media. J. Contam. Hydrol. 43, 129–146.
Araujo, J.B., Mainhagu, J., Brusseau, M.L., 2015. Measuring air-water interfacial area for soils using the mass balance surfactant-tracer method. Chemosphere 134, 199–202.
Araujo, J.B., Brusseau, M.L., 2019. Assessing XMT-Measurement variability of air-water interfacial areas in natural porous media. Water Resour. Res. 55.
Barnes, G., Gentle, I., 2005. Interfacial Science: an Introduction. Oxford University Press, New York, NY.
Brusseau, M.L., Popovicova, J., Silva, J.A.K., 1997. Characterizing gas-water interfacial and bulk-water partitioning for gas-phase transport of organic contaminants in unsaturated porous media. Environ. Sci. Technol. 31, 1645–1649.
Brusseau, M.L., Peng, S., Schaar, G., Costanza-Robinson, M.S., 2006. Relationships among air-water interfacial area, capillary pressure,and water saturation for a sandy porous medium. Water Resour. Res. 42, W03501.
Brusseau, M.L., Peng, S., Schnaar, G., Murao, A., 2007. Measuring air-water interfacial areas with X-ray microtomography and interfacial partitioning tracer tests. Environ. Sci. Technol. 41, 1956–1961.
Brusseau, M.L., Janousek, H., Murao, A., Schnaar, G., 2008. Synchrotron X-ray microtomography and interfacial partitioning tracer test measurements of NAPL-water interfacial areas. Water Resour. Res. 44, W01411.
Brusseau, M.L., El Ouni, A., Araujo, J.B., Zhong, H., 2015. Novel methods for measuring air-water interfacial area in unsaturated porous media. Chemosphere 127, 208–213.
Costanza-Robinson, M.S., Brusseau, M.L., 2002. Air-water interfacial areas in unsaturated soils: evaluation of interfacial domains. Water Resour. Res. 38 (10), 1195.
Costanza-Robinson, M.S., Harrold, K.H., Lieb-Lappen, R.M., 2008. X-ray microtomography determination of air-water interfacial areawater saturation relationships in sandy porous media. Environ. Sci. Technol. 42 (8), 2949–2956.
Costanza-Robinson, M.S., Zheng Zheng, E. J. Henry, Estabrook, B.D., Littlefield, M.H., 2012. Implications of surfactant-induced flow for miscible-displacement estimation of air–water interfacial areas in unsaturated porous media. Environ. Sci. Technol. 46 (20), 11206–11212.
Culligan, K.A., Wildenschild, D., Christensen, B.S.B., Gray, W.G., Rivers, M.L., Tompson, A.F.B., 2004. Interfacial area measurements for unsaturated flow through a porous medium. Water Resour. Res. 40, W12413.
Dobson, R., Schroth, M.H., Oostrom, M., Zeyer, J., 2006. Determination of NAPL-water interfacial areas in well-characterized porous media. Environ. Sci. Technol. 40, 815–822.
Guo, B., Zeng, J., Brusseau, M.L., 2020. A Mathematical model for the release, transport, and retention of per- and polyuoroalkyl substances (PFAS) in the vadose zone. Water Resour. Res. 56 article e2019WR026667.
Jiang, H., Guo, B., Brusseau, M.L., 2020. Pore-scale modeling of fluid-fluid interfacial area in variably saturated porous media containing micro-scale surface roughness. Water Resour. Res. 56 article: e2019WR025876.
Kauck, E.A., Diesslin, A.R., 1951. Some properties of perfluorocarboxylic acids. Ind. Eng. Chem. 43, 2332–2334.
Kim, H., Rao, P.S.C., Annable, M.D., 1997. Determination of effective air-water interfacial area in partially saturated porous media using surfactant adsorption. Water Resour. Res. 33 (12), 2705–2711.
Kim, H., Rao, P.S.C., Annable, M.D., 1999. Gaseous tracer technique for estimating air-water interfacial areas and interface mobility. Soil Sci. Soc. Am. J. 63, 1554–1560.
Kim, H., Annable, M.D., Rao, P.S.C., 2001. Gaseous transport of volatile organic chemicals in unsaturated porous media: effect of water partitioning and air-water interfacial adsorption. Environ. Sci. Technol. 35, 4457–4462.
Lyu, Y., Brusseau, M.L., Ouni, A.E., Araujo, J.B., Su, X., 2017. The gas-absorption/chemical-reaction method for measuring air-water interfacial area in natural porous media. Water Resour. Res. 53, 9519–9527.
Lyu, Y., Brusseau, M.L., Chen, W., Yan, N., Fu, X., Lin, X., 2018. Adsorption of PFOA at the air–water interface during transport in unsaturated porous media. Environ. Sci. Technol. 52, 7745–7753.
McDonald, K., Carroll, K.C., Brusseau, M.L., 2016. Comparison of fluid-fluid interfacial areas measured with X-ray microtomography and interfacial partitioning tracer tests for the same samples. Water Resour. Res. 52 (7), 5393–5399.
Or, D., Tuller, M., 1999. Liquid retention and interfacial area in variably saturated porous media: upscaling from single-pore to sample-scale model. Water Resour. Res. 35 (12), 3591–3605.
Peng, S., Brusseau, M.L., 2005. Impact of soil texture on air-water interfacial areas in unsaturated sandy porous media. Water Resour. Res. 41, W03021.
Saripalli, K.P., Kim, H., Rao, P.S.C., Annable, M.D., 1997. Measurement of specific fluid-fluid interfacial areas of immiscible fluids in porous media. Environ. Sci. Technol. 31, 932–936.
Schaefer, C.E., DiCarlo, D.A., Blunt, M.J., 2000. Experimental measurement of air-water interfacial area during gravity drainage and secondary imbibition in porous media. Water Resour. Res. 36 (4), 885–890.
Willson, C.S., Lu, N., Likos, W.J., 2012. Quantification of grain, pore, and fluid microstructure of unsaturated sand from x-ray computed tomography images. Geotech. Test J. 35 (6), 911–923.